Journal of Chromatography A, 1217 (2010) 8257–8269

Contents lists available at ScienceDirect

Journal of Chromatography A

journal homepage: www.elsevier.com/locate/chroma

A new multicolumn, open-loop process for center-cut separation by solvent-gradient chromatography

Ricardo J.S. Silva[a], Rui C.R. Rodrigues[a], Hector Osuna-Sanchez[b], Michel Bailly[c], Eric Valéry[b], José P.B. Mota[a,*]

[a] Requimte/CQFB, Departamento de Química, Faculdade de Ciências e Tecnologia, Universidade Nova de Lisboa, 2829-516 Caparica, Portugal
[b] NOVASEP Process, Boulevard de la Moselle, BP 50, 54340 Pompey, France
[c] Laboratoire de Réactions et Génie des Procédés, ENSIC-INPL, 1 rue Grandville, B.P. 451, 54001 Nancy Cedex, France

ARTICLE INFO

Article history:
Received 2 September 2010
Received in revised form 28 October 2010
Accepted 1 November 2010
Available online 9 November 2010

Keywords:
Center-cut separation
Solvent gradient
Multi-column chromatography
Open-loop configuration
Biochromatography

ABSTRACT

A comprehensive description of a new process—the GSSR (Gradient with Steady State Recycle) process—for center-cut separation by solvent-gradient chromatography is provided, highlighting its versatility, flexibility, and ease of operation. The GSSR process is particularly suited for ternary separation of bioproducts: it provides three main fractions or cuts, with a target product contained in the intermediate fraction. The process comprises a multicolumn, open-loop system, with cyclic steady state operation, that simulates a solvent gradient moving countercurrently with respect to the solid phase. However, the feed is always injected into the same column and the product always collected from the same column as in a batch process; moreover, both steps occur only once per cycle. The GSSR process was experimentally validated in a pilot unit, using the purification of a crude peptide mixture by reversed phase as a proof of concept; the crude mixture is roughly 50% pure and some of its impurities have isocratic retention times very close to that of the target peptide. Experimental results are reported in terms of cyclic steady-state profiles and process performance indicators, which include product purity and yield. A simplified model-based approach, which uses only a few key components of the crude mixture, is employed to assist in the explanation of the process operation. By dynamically adjusting the switching interval while the process is running, to correctly position the composition profile with respect to the outlet ports, pure product satisfying the target specifications—98% purity and 95% recovery—was obtained under stable operation in the pilot unit.

1. Introduction

The advances in biotechnology and developments in genetic engineering have resulted in the scale up and manufacturing of biopharmaceutical products [1]. Today, downstream processing is facing the challenge of manufacturing products with the highest degrees of purity and integrity, and overall process economy, while keeping pace with the rapidly increasing upstream yields in biotechnology. The fulfillment of the strict requirements by downstream purification is the major cost factor in biotechnological production with 50–80% of the total manufacturing cost [2].

A major part of the purification costs is related to chromatographic processes, which, at present, are still largely operated in batch mode. This is not because chromatography is inherently expensive, but because it is heavily used: chromatography plays a central role in fast and efficient separation of biochemical and pharmaceutical compounds; in fact, it still remains the work horse method in biopurification.

For most biopurification problems, the desired product is intermediate between weakly and strongly adsorbing impurities, and a central cut is thus required to get the desired product. Conventionally, the generic three-fraction biopurification problem is solved using batch column chromatography, often incorporating solvent gradients. Typically, the target product is separated from process-related impurities through a series of steps wherein a selected cut or fraction of the effluent from the previous step is selectively adsorbed and desorbed onto a given stationary phase using time and elution conditions as manipulated variables, until, ultimately, yielding the product purified to the desired level. Solvent gradients are easy to apply in sequential batch chromatography, but this operating mode suffers from high product dilution, low efficiency and productivity, and high solvent consumption.

As a general rule, multicolumn processes combining freely adjustable, smooth gradients and simulated countercurrent (SCC) adsorption can achieve better performance than sequential batch chromatography. Early studies [3–6] on ternary separation by

* Corresponding author. Tel.: +351 212948385; fax: +351 212948385.
E-mail address: pmota@dq.fct.unl.pt (J.P.B. Mota).

0021-9673/$ – see front matter © 2010 Elsevier B.V. All rights reserved.
doi:10.1016/j.chroma.2010.11.005

isocratic SCC chromatography were focused on continuous processes (i.e., with continuous feeding and product withdrawal) and showed that this restrictive design criterium can only be achieved with column configurations comprising several fluid zones (here, a zone refers to the columns between two active ports). The most commonly explored column configurations have been simulated moving-bed (SMB) cascades [4,7] and five-zone systems with side streams [8–11].

Bioseparation, on the other hand, does not require that the separation scheme be continuous; this allows several possibilities and a multitude of operating modes to be considered in the design of the process, which otherwise would have to be excluded. In principle, a semi-continuous, multicolumn process can make use of various techniques to achieve the desired separation; for example, some columns can be dynamically interconnected, so that non-pure product cuts are internally and countercurrently recycled, while other columns can be short circuited to operate in pure batch mode, and others frozen to introduce time lags between the positions of the various concentration fronts. This way some fractions can be separated by a SCC approach (the mass-transfer zone is kept inside the system by means of the port switching and the remixing with the feed), whereas the separation of other fractions can be chromatographic (the mass-transfer zone is taken out of the system). By freezing one or more columns (i.e., stopping the flow through them) for some steps of the cycle, it is possible to decouple the migrating velocities of the various solutes.

The schemes developed by Jin and Wankat [12,13] and by our group [14–17] are examples of existing processes for isocratic binary separation that combine some of the techniques above into a single hybrid scheme. The case of isocratic ternary separation is clearly more complicated. The idea of operating only partially in a countercurrent fashion was exploited by Masuda et al. [18] in a single cascade process for fractional separation that is commercialized by Organo Corp., Tokyo, Japan; the performance of this process has been analyzed by other authors [19–21]. Hur and Wankat [22] developed a two-zone SMB/chromatography hybrid system for ternary separations, and compared its performance to those of cascades of two-zone and four-zone SMBs. Subsequently, the same authors [23] designed a semi-continuous, center-cut, two-zone SMB/chromatography system and a recycled cascade with two four-zone SMBs to separate the intermediate component from ternary mixtures.

Recently, Morbidelli and co-workers [24–29] developed a chromatographic process for ternary separation (MCSGP-process) that exploits the power of gradient chromatography and hybrid SMB/chromatography modes. In this process some columns operate in counter-current mode during a fraction of the cycle while others are short-circuited and operate in batch mode. Continuous operation of the MCSGP requires six columns [24,27], but the process can be reduced to a fully equivalent semi-continuous configuration with only three chromatographic columns and three gradient pump modules [28,29]. Using a series of working examples, these authors have demonstrated the superiority of MCSGP over batch chromatography.

In the present work, we describe a new multicolumn, open-loop process for center-cut separation by solvent-gradient chromatography. The key idea is to extend solvent-gradient batch chromatography to a train of columns and to exploit the fractionation of the stationary phase. In single-column batch chromatography the product and waste cuts are obtained at the same point in the system—at the downstream end of the column—but at different times. Therefore, time (or elution volume) is the only variable for defining the fractional cuts. If a solvent gradient is used, it is introduced into the system at a single point—the upstream end of the column. This, of course, does not give much freedom for dynamically adjusting the solvent composition profile inside the column.

Although packing the stationary phase into a single column works fine for many binary separations, this seems to be overly restrictive for center-cut separations. The introduction of space as an additional variable (although being a discrete one), by dividing the stationary phase into a train of columns, adds more flexibility for manipulating the cuts and for generating the solvent gradient; furthermore, with such a column arrangement it is possible to recycle some of the cuts from the downstream end of the system to its upstream end.

In this work we show that this can be done while working in a simple, open-loop system that resembles the batch system. Although our process implements a solvent-gradient moving around a ring of columns, it is similar to a batch process in terms of feeding and product collecting. We provide experimental validation in a pilot unit, using the purification of a crude peptide mixture by reversed phase as a working example; this proof of concept serves to highlight the versatility, flexibility, and ease of operation of the process.

2. Process description

The new process, nicknamed GSSR (Gradient with Steady State Recycle), comprises a multi-column, open-loop system, with cyclic steady-state operation, that simulates a solvent gradient moving countercurrently with respect to the solid phase. It is particularly suited for ternary separations: it provides three main fractions or products, with a target product contained in the intermediate fraction. The process can be pictured as the superposition of three steady periodic events applied to a ring of columns with an open-loop configuration: a moving solvent gradient, a feeding step, and a step of product collection. A comprehensive description of the GSSR process is provided next.

First, consider how a moving solvent gradient is implemented by means of a plurality of solvent lines. For this purpose, consider the schematic of Fig. 1, which is an example of the simplest GSSR sequence applied to a three-column train. Note, however, that the process can operate with more columns. The three-column train of Fig. 1 is supplied with three different solvents: solvent A, which has a linear-gradient composition, and two isocratic solvents, B and C, with elution strengths different from A.

The inlet positions and flow rates of the solvent lines are defined for a single switching interval as a set of steps over that period of time. The sequence is then repeated a number of times equal to the number of columns, the only difference between a switching interval and the next being the shift of the solvent inlets by one column in the direction of the fluid flow. A complete cycle is defined by the sequence of steps for the set of switching intervals.

From this description, it follows that the inlet positions and flow rates of the solvent lines are periodic in time, with period τ, where τ is the duration of a switching interval. There is always an open outlet, which is taken as a waste fraction, in order to keep the system in open loop. The net effect of this cyclic scheme is the simulation of the counter-current movement of the solid phase relative to an open-loop solvent gradient that is τ-periodic in time.

If the system is operated for a large number of cycles, the solvent will develop a steady, τ-periodic, axial composition profile extending over the columns. Note that the solvent composition profile will not be spatially periodic (i.e., it will not be periodic along a coordinate extending from the upstream end of the first column to the downstream end of the last column), but only time periodic; for the profile to be spatially periodic, all columns would have to be supplied with the same solvent gradient.

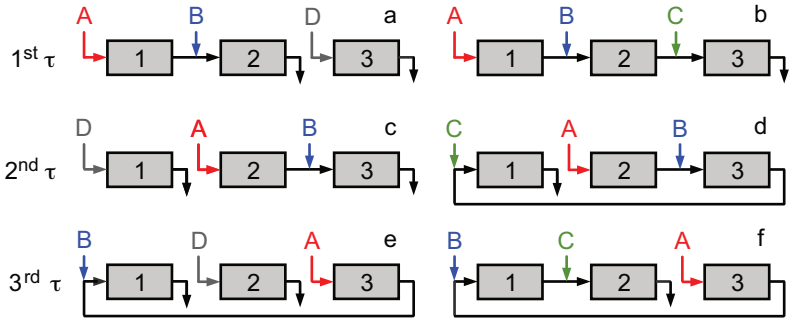

Fig. 1. Basic sequencing of the solvent lines for a three-column GSSR process. The righthand sequence—steps b, d, and f—is for operation without on-line regeneration or cleaning in place. A sequence with desorption zone consists of performing the lefthand step for an initial fraction, say α, of the corresponding switching interval, followed by its righthand counterpart for the remaining $(1-\alpha)$. All active outlets are diverted to waste.

In biochromatography a suitable regeneration method is essential for maximizing column performance and obtaining reproducible results. The regeneration usually entails the use of a strong solvent to remove highly adsorbed impurities, and may require post-equilibration of the column with regular buffer. For this purpose, the GSSR process provides the possibility for in-line regeneration or cleaning in place (CIP) by dividing the switching interval into two sub-steps and replacing solvent C by a stronger solvent D over the first sub-step. Thus, during an initial fraction, say α, of each switching interval, the column whose upstream end is attached to the active inlet line of solvent C is partially or totally flushed with solvent D; during this time, the addition of solvent C is halted. Moreover, while the column is desorbed with solvent D, the outlet effluent of the upstream column is diverted to waste. Once the initial sub-step of the switching interval is completed, the two columns resume their normal operation. It is worth noting that nothing has yet been said about feeding and product collecting; thus, for the moment all active outlets (e.g., those depicted in Fig. 1) should be interpreted as waste outlets.

In order to establish a GSSR cycle, two additional steps must be defined: (i) the time interval during which fresh feed is supplied into the system; and (ii) the time interval during which the target product is collected. These two steps are cyclic, but take place only once per cycle, i.e., they are both $N\tau$-periodic, where N is the number of columns. Moreover, they can be applied anywhere within the cycle and can cross or extend over consecutive switching intervals; depending on the difficulty of separation, the feed injection and product withdrawal can be performed over different intervals of the cycle, or they can take place at the same time, or they can partially overlap. However, the feed is always injected into the same column as a rectangular pulse and the product is always collected from the same column.

In order to explain how the feed and production steps work in a GSSR process, let us consider again a three-column ring, such as the one shown in Fig. 1. For difficult separations—those in which the target product is surrounded by closely eluting impurities—the feeding and product collecting should occur at opposite ends of the ring to establish the longest path between the feed inlet and the product outlet, and thus help to separate the impurities nearest to the target component. Without loss of generality, it will be assumed that the feed line is connected to the inlet of column 1 and the product line connected to the outlet of column 3.

Since in many cases the target solute will not be completely separated from its two nearest neighbor impurities when it reaches the collection point at the downstream end of the ring, the two impure cuts surrounding the purified product—one containing the leading edge of the target component and the other the trailing edge—must be recycled to the feed point at the upstream end of the system in order to maximize the recovery rate. For optimal performance, the two mixed cuts must be recycled in such a way as to surround the feed pulse loaded into the feed column. Therefore, for difficult separations that require this recycling strategy the feed and product withdrawal steps must necessarily overlap. Moreover, to get the most efficient separation the feed pulse should be moved through the system by the moving solvent gradient (A) and not eluted isocratically with either solvent B or C.

From this discussion it is now clear when to carry out the feed and production steps within the sequencing of the solvent lines shown in Fig. 1 for the case where the feed line is connected to inlet of column 1 and the product line connected to the outlet of column 3: the two steps must take place somewhere in the time interval of the cycle spanned by steps d, e, and f of Fig. 1, because during these steps the effluent from column 3 is recycled to the upstream end of column 1. Given that steps d and f have the same duration, combining the collection of the target peak with step e is a simple and pragmatic solution that places the product collection in the middle of the recycling sequence. Moreover, by feeding in step e the mixture is injected into the correct column, which is the one that is afterwards eluted with the solvent gradient.

There is one last detail to take into account regarding the feed and production steps. If the feed step is shorter than the production step, column 1 should be frozen after the feed step while the product is still being withdrawn from column 3, so that when the mixed cut containing the trailing edge of the product is recycled to the upstream end of column 1 it is placed next to the feed cut.

Fig. 2 shows the flow diagrams of the feed and production steps for the case when they occur at the beginning of the third switching interval, as discussed above, and when the product withdrawal

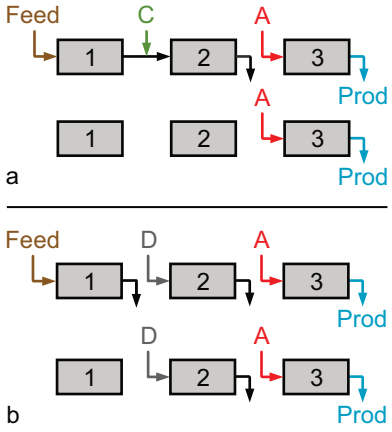

Fig. 2. Flow diagrams of the feed and production steps for the case when they occur at the beginning of the third switching interval and when the product withdrawal takes longer than the injection of feed. Schematics (a) and (b) are for operations with and without on-line regeneration or cleaning in place, respectively. When the production step is finished the normal operation of the train of solvents is resumed.

takes longer than the injection of feed; the two sub-cases of operation with and without CIP must be handled separately and require different flow diagrams. When the production step is finished the normal operation of the train of solvents is resumed. Other cases of placement of the feed and production steps in the GSSR cycle are discussed elsewhere [30].

Before concluding this section, it is worth noting that, in practice, the solvent gradient does not strictly follow the rules for simulating its counter-current movement around the ring of columns, but only approximately, due to the interference of the feeding and product collecting. The precise simulation of the counter-current movement of the solid is given up in favor of the extra flexibility provided by our cycle. Also, because the points of feeding and product collecting are fixed, each column can play a unique role in the separation. For the same reason, the N switching intervals that comprise a full GSSR cycle will not necessarily have the same length. This is different from multi-column systems adhering strictly to the simulated counter-current concept, where all columns undergo the same sequence of steps but phase out in time by multiples of the same switching interval, and opens up opportunities for a whole new range of cycles.

3. Experimental

3.1. Pilot unit

Fig. 3 shows a schematic flowsheet of the GSSR pilot unit. We use a distributed valve design based on two-way valves, since they are quite versatile and make it possible to implement independent port switching. Two-way valves allow the flow either to go through or not to go through. The two-way valves are model SFVO from Valco International (Schenkon, Switzerland) with pneumatic actuation. Each valve is automated by means of a single computer-controlled, three-way solenoid: application of 50 psi opens the valve; venting the air allows the spring to return the valve to the closed position. Overall, the pilot unit employs 28 two-way valves.

Each set of six valves, $\{v^{CO}, v^{A1}, v^{A2}, v^{B}, v^{C}, v^{D}\}_j$ ($j = 1, 2, 3$), is connected to a special tee with six inlets and one outlet; a check valve is placed in front of valve v^{CO} to prevent the occurrence of flow reversal. The other valves are attached to the transfer lines between columns by regular tees.

By simultaneously closing valve v_j^{CO} ($=0$) and opening valve v_j^{W} ($=1$), the effluent from column j is directed to the corresponding waste line; similarly, by simultaneously closing valve v_3^{CO} ($=0$) and opening valve v^{P} ($=1$), the effluent from column 3 is directed to the product line.

3.1.1. Inlet flow rates

The GSSR process employs three isocratic solvent streams—B, C, and D—with different solvent compositions, and one solvent-gradient stream, A. The composition of the solvent-gradient stream is τ-periodic in time and is continuously supplied into the process at constant flow rate Q_A. Solvents B and C are fed to the process at constant flow rates Q_B and Q_C, respectively; their flows, however, may have to be temporarily stopped while feeding or collecting product. Solvent D replaces solvent C during the desorption step of every switching interval; its flow rate, Q_D, is constant. Finally, the feedstock fluid is injected once per cycle as a rectangular pulse with flow rate Q_F. Overall, the inlet flow rates of the GSSR process are either constant or on/off; in the latter case, the flow rate is kept constant, at 0 or Q, over a given time interval before jumping discretely to the other value, Q or 0, over the next interval.

The HPLC pumps for the solvent lines B, C, and D, as well as that for the feed line, F, are operated under steady conditions at their prescribed flow rates to minimize disturbances in their operation. To interrupt the feed flow or the flow of one of the isocratic solvent streams, say stream B, the control software closes valve v_j^{B} and opens valve v^{Bn} to redirect the flow back to the solvent storage tank. Since for all purposes the valve switching is instantaneous, the net effect is a very good approximation of the sharp edge of the step change in the flow rate. To redirect the flow of solvent B to column j, valve v^{Bn} is closed and valve v_j^{B} is open; the sharp edge of the step change in the flow rate is well reproduced again. The valves which are employed for redirecting the flow of an inlet line back to its source tank are v^{Fn}, v^{Bn}, v^{Cn}, and v^{Dn}.

Over each switching interval, the composition of solvent A changes linearly with time from $c_A^{(0)}$ to $c_A^{(\tau)}$,

$$c_A(t) = c_A^{(0)} + \frac{c_A^{(\tau)} - c_A^{(0)}}{\tau}(t \bmod \tau), \tag{1}$$

where $(\cdot \bmod \cdot)$ is the modulo operator, i.e., $(t \bmod \tau) \equiv t - \tau \cdot \mathrm{int}(t/\tau)$. In the pilot unit, the solvent-gradient line is mimicked by the admixture of two isocratic solvent streams, A1 and A2, driven by two variable-velocity isocratic pumps, with two different solvent compositions, respectively, c_{A1} and c_{A2}, that satisfy $c_{A1} \le \min\{c_A^{(0)}, c_A^{(\tau)}\}$ and $c_{A2} \ge \max\{c_A^{(0)}, c_A^{(\tau)}\}$. To reproduce the solvent gradient by the admixture of streams A1 and A2, the flow rates of the two HPLC pumps, Q_{A1} and Q_{A2}, are determined from the following material balances:

$$Q_{A1} + Q_{A2} = Q_A, \tag{2}$$

$$Q_{A1}c_{A1} + Q_{A2}c_{A2} = Q_A c_A. \tag{3}$$

It is easily shown that $Q_{A1}(t)$ and $Q_{A2}(t)$ are τ-periodic, linear functions of time:

$$Q_{A1}(t) = Q_{A1}^{(0)} + \frac{Q_{A1}^{(\tau)} - Q_{A1}^{(0)}}{\tau}(t \bmod \tau), \tag{4}$$

$$Q_{A2}(t) = Q_{A2}^{(0)} + \frac{Q_{A2}^{(\tau)} - Q_{A2}^{(0)}}{\tau}(t \bmod \tau), \tag{5}$$

where

$$Q_{A1}^{(0)} = Q_A \frac{c_A^{(0)} - c_{A2}}{c_{A1} - c_{A2}}, \quad Q_{A1}^{(\tau)} = Q_A \frac{c_A^{(\tau)} - c_{A2}}{c_{A1} - c_{A2}}, \tag{6}$$

$$Q_{A2}^{(0)} = Q_A \frac{c_A^{(0)} - c_{A1}}{c_{A2} - c_{A1}}, \quad Q_{A2}^{(\tau)} = Q_A \frac{c_A^{(\tau)} - c_{A1}}{c_{A2} - c_{A1}}. \tag{7}$$

The six HPLC pumps employed in the pilot plant are model K-501 from Knauer (Berlin, Germany) with 10 mL and 50 mL pump heads, commanded by RS232 communication protocol.

3.1.2. Monitoring and fraction collection

A multi-wavelength UV detector (USB2000 from Ocean Optics, USA) with attenuator, connected to a DH-2000-S-DUV light source (Micropack, Ostfildern, Germany), is attached to the outlet of column 3. The communication between the UV detector and the control software is handled via a USB connection.

A fraction collector is also installed at the outlet of column 3, after the UV detector, for the periodic collection of internal samples that can be later analyzed by off-line HLPC. Each fraction is collected into a vial using an electrically driven, six-port, two-position valve, model K6 from Knauer (Berlin, Germany), commanded by RS232 communication protocol.

Most of the time, the effluent from column 3 flows through the UV measuring cell and through the injection loop of the six-port valve and is (i) directed to column 1, or (ii) collected as product, or (iii) removed as waste. At selected times the six-port valve is switched to 'inject position' and valve v^{FC} is open, to place the injection loop within the flow path of mobile phase from a pressurized tank. The sample in the injection loop is thus pushed onto

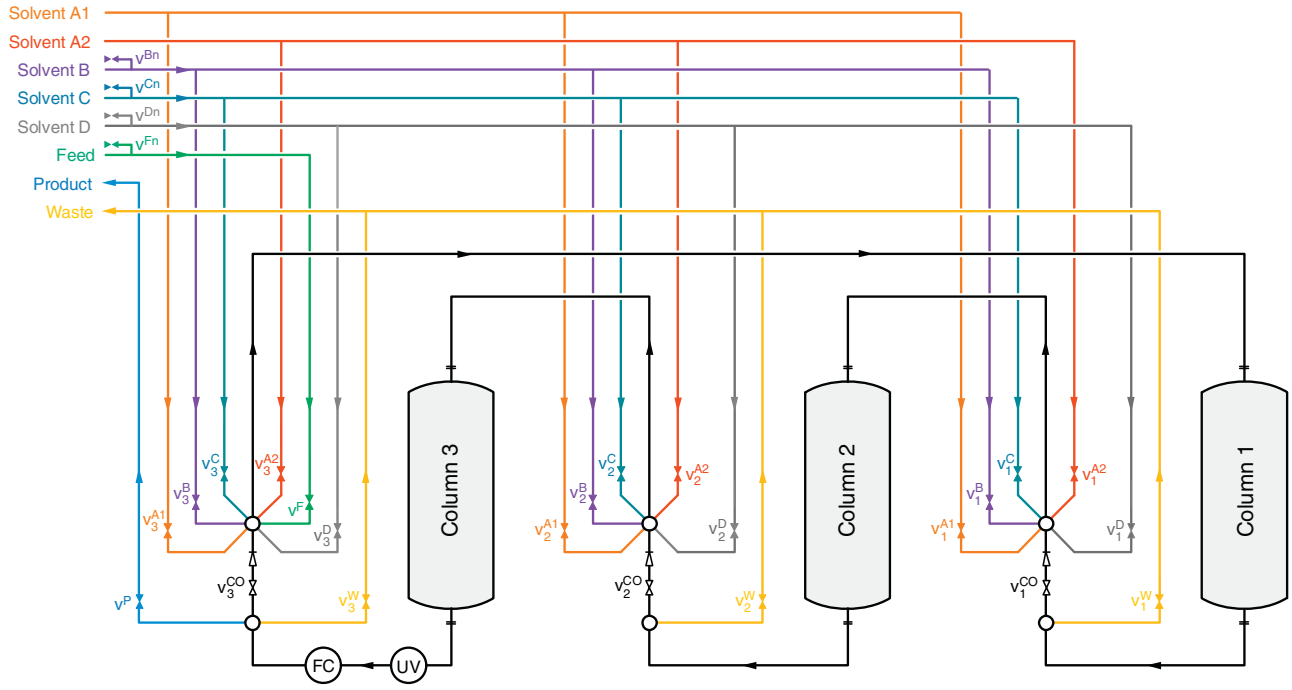

Fig. 3. Schematic flowsheet of the GSSR pilot unit. v_j^{α}, two-way valve; UV, UV detector; FC, fraction collector.

the vial for off-line HPLC analysis and the injection loop is washed with mobile phase. This occurs during a small, specified time interval at given instants of the cycle defined by the operator. During this time the effluent from column 3 bypasses the injection loop and is directly diverted into column 1. When the six-port valve is switched back to 'load' position and valve v^{FC} is closed, the mobile phase in the loop is pushed to the downstream column while the loop is being filled. Thus, the circulating flow in the pilot unit is not interrupted. The extra volumes in the pilot unit due to ancillary equipment, tubbing, detectors, and fraction collector were estimated to be 4.5 mL.

3.1.3. Process automation

The whole set-up, including pumps, two-way valves, UV detector, and fraction collector, is fully automated and driven by BioCTR [31]—our Labview-based software for process monitoring and control of multicolumn chromatographic processes.

A GSSR cycle is defined by a set of parameters, which are specified by the operator and can be changed while the pilot is running. Besides the number of columns, N, switching interval, τ, and the various flow rates, the set of operating parameters for a GSSR cycle includes other parameters that are described next. The start of the feed injection, t_F, is defined relative to the cycle time, $\tau_{cyc} = N\tau$, as t_F/τ_{cyc}, but the duration of the injection, Δt_F, is defined in absolute time units. Product collection is defined similarly; hence, t_P/τ_{cyc} is the relative position of the start of collection and Δt_P specifies its duration.

The GSSR process can operate with a desorption zone where solvent C is replaced by a stronger solvent D. This step is applied once per switching interval and, therefore, is best defined with respect to that time interval. During the initial interval $0 \le t/\tau < \Delta t_D/\tau$ of every switching interval the system is operated with solvent D, whereas during the rest of the period, $\Delta t_D/\tau \le t/\tau < 1$, solvent D is replaced by normal solvent C. The solvent-gradient parameters Q_A, $c_A^{(0)}$, and $c_A^{(\tau)}$ are automatically converted by the control software into the flow rate parameters $Q_{A1}^{(0)}$, $Q_{A1}^{(\tau)}$, $Q_{A2}^{(0)}$, and $Q_{A2}^{(\tau)}$, using Eqs. (6) and (7).

3.2. Materials and methods

The GSSR process was experimentally validated on the pilot unit, using the reversed-phase purification of a crude peptide mixture as a working example. Proteins and peptides represent a growing sector in the pharmaceutical industry. Reversed-phase, high-performance liquid chromatography (RP-HPLC) has found wide use in the production of peptides for pharmaceutical formulations, due to its ability to provide high-resolution separation combined with good reproducibility. However, peptide mixtures can be complex, with significantly heterogeneous physico-chemical properties (including hydrophobic and highly hydrophilic compounds), thus rendering their efficient separation by RP-HPLC challenging [32]. Here, we demonstrate that the GSSR process is well suited for this task at preparative scale.

The selected packing material is Kromasil C18 (Eka Chemicals AB, Sweden), an octadecyl-bonded, reversed-phase silica, with high hydrophobicity, narrow pore size distribution (~100 Å), and very low content of metal impurities. Detrimental ionic interactions between basic peptides and residual ionized silanol groups in C18 phases often produce peak tailing [33,34], which is undesirable when high product purity is required; the Kromasil C18 phase has a high graft density and end-capping, and is therefore expected to exhibit a low silanol activity under the selected experimental conditions. The analytical experiments were performed with 5 μm Kromasil C18 purchased prepacked into a 0.46 cm × 15 cm column; the preparative experiments were performed with 25 μm Kromasil C18, packed into three 1 cm × 10 cm stainless steel columns by NOVASEP Process (France). The system was operated isothermally at 30 °C.

The mobile phases used in this study are aqueous solutions of ethanol (EtOH) with a fixed residual amount of 0.1% (v/v) terephthalic acid (TFA); the EtOH concentrations varied from 20% up to 50% (v/v). HPLC-grade EtOH and TFA were purchased from Panreac (Barcelona, Spain). The EtOH buffers were first prepared by diluting EtOH in deionized water, filtering through a 0.22-μm membrane, and adding TFA thereafter to prepare the final mobile phases. All solvents were degassed prior to use.

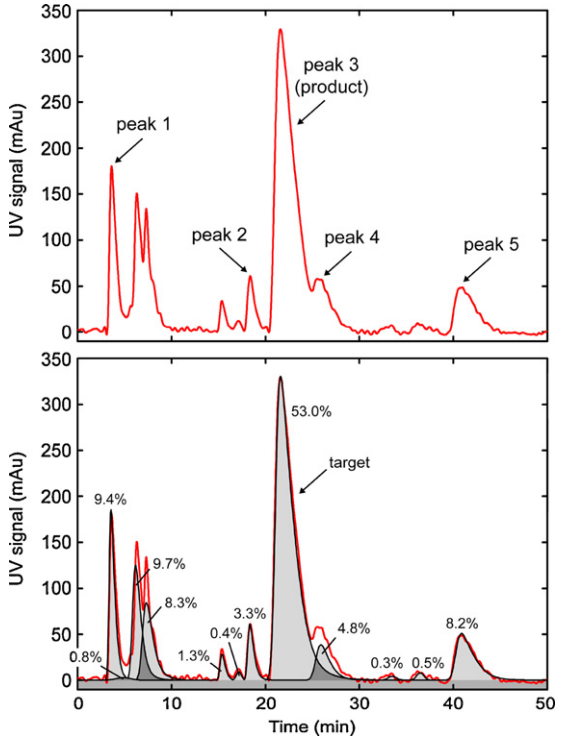

Fig. 4. Peak deconvolution for an analytical chromatogram of the crude peptide mixture. Column: Kromasil C18, 5 μm, 100 Å, 0.46 cm × 15 cm; solvent: water/ethanol/TFA (75/25/0.1, % (v/v)); flow rate: 0.5 mL/min; concentration: 1 g/L; injected volume: 250 μL; detector: UV @ 220 nm.

Fig. 4 shows a chromatogram of the crude mixture for a 250 μL injection at 1 g/L into the Kromasil analytical column, eluted with water/ethanol/TFA (75/25/0.1, % (v/v)) at 0.5 mL/min. The crude mixture is characterized by three main cuts: a weakly adsorbing (early eluting) cut containing three major impurities, an intermediate cut with the target product and at least four neighboring impurities, and a strongly adsorbing (late eluting) cut containing three impurities; the target product corresponds to the largest peak of the chromatogram, with roughly 50% of the total peak area. From the analysis of the chromatogram in Fig. 4, it is clear that the desired product is intermediate between nearby, weaker and stronger adsorbing impurities; a central cut is thus required to get the desired pure product.

4. Model-based analysis tools

For the sake of simplicity, we shall employ a linear adsorption model to help explain the operation of the GSSR process for the purification of the peptide crude mixture. A comprehensive, numerical study of the GSSR process, based on a more realistic multicomponent adsorption model of the peptide mixture, will be reported elsewhere.

The adsorption equilibrium of the competing solutes is the basis for the design or optimization of any chromatographic process governed by the thermodynamics of adsorption; this is the case of the peptide mixture on the 25 μm Kromasil C18 phase for the working range of linear velocities used in the preparative experiments. Mass transfer and axial dispersion certainly influence the composition fronts, by smearing the concentration profiles, but do not change their stoichiometric positions when the process is not limited by the adsorption kinetics. If the adsorption isotherms are known, suitable operating conditions can be determined through the application of design rules, such as those developed for the SMB process [35], or by computer-aided optimization. A short-cut method for designing the GSSR cycle is presented below.

4.1. Chromatographic column model

Under linear adsorption conditions, the equilibrium adsorbed concentrations can be expressed as

$$q_i = (\epsilon_p + H_i)c_i, \tag{8}$$

where i is the solute index; c is the concentration in the liquid phase; q is the adsorbed concentration per unit volume of stationary phase; ϵ_p is the intraparticle porosity; and H is the Henry's constant. Henceforth index $i=0$ shall denote the solvent modifier (EtOH) and $i=1,\ldots,n_c$, the n_c components of the peptide mixture.

The Henry's constant is strongly affected by the solvent composition; examples of expressions often used in the literature to model the dependence of H_i on c_0 are [36–38]

$$H_i = \frac{H_i'}{c_0^{n_i}} \quad \text{and} \quad H_i = \frac{H_i'}{e^{n_i c_0}}, \tag{9}$$

where H_i' and n_i are adjustable parameters.

For simplicity, we use the equilibrium-dispersed model for describing the dynamics of each chromatographic column [39]. If the dependence of H_i on c_0 is given by $H_i = H_i'/c_0^{n_i}$, the equilibrium-dispersed model can be written as

$$\left(\epsilon + \frac{V_e}{V}\right)\frac{\partial c_i}{\partial t} + K_i\left(\frac{\partial c_i}{\partial t} - \frac{n_i c_i}{c_0}\frac{\partial c_0}{\partial t}\right) = \frac{Q}{V}\left(\frac{h_i}{2}\frac{\partial^2 c_i}{\partial x^2} - \frac{\partial c_i}{\partial x}\right), \quad \times 0 < x < 1, \tag{10}$$

with boundary conditions

$$c_i - \frac{h_i}{2}\frac{\partial c_i}{\partial x} = c_i^{in} \quad \text{for } x = 0, \tag{11}$$

$$\frac{\partial c_i}{\partial x} = 0 \quad \text{for } x = 1. \tag{12}$$

In these equations, $\epsilon = \epsilon_b + (1-\epsilon_b)\epsilon_p$ is the total bed porosity (ϵ_b is the interparticle void fraction); $K_i = (1-\epsilon_b)H_i$, the Henry's constant expressed per unit volume of column; t, the time coordinate; $x = z/L$, the dimensionless axial coordinate along the column; L and V, the length and volume of the column; V_e is the extra dead volume per column; Q, the flow rate through the column; h, the dimensionless plate height; and c^{in}, the solute concentration in the inlet effluent. The lefthand side of Eq. (10) is the expansion of $\epsilon_b(\partial c_i/\partial t) + (1-\epsilon_b)(\partial q_i/\partial t)$. Note that for $i=0$ (EtOH in the solvent), we have set $H_0' = 0$ and $n_0 = 0$.

The dimensionless plate height, h_i, governing band broadening for the i th component, can be expressed as [40]

$$\frac{h_i}{2} = \frac{1}{Pe} + \alpha_i\frac{Q}{V} + \gamma_i\frac{V}{Q}, \tag{13}$$

where

$$\alpha_i = \frac{\epsilon - \epsilon_b + K_i}{k_i(\epsilon + K_i)^2}, \quad \gamma_i = \frac{\epsilon_b D_{im}}{\alpha_b L^2}. \tag{14}$$

Here, $Pe = \nu L/D_L$ is the hydrodynamic Péclet number ($D_L \propto d_p\nu$ is the hydrodynamic dispersion coefficient and d_p is the particle diameter); $k \propto d_p^{-2}$ is the linear-driving-force coefficient for lumped solid-diffusion mass transfer (including film diffusion); D_m is the molecular diffusion coefficient; and $\alpha_b \approx 3$ is the tortuosity factor of the packed bed. Note that γ measures the effect of bulk molecular diffusion on band broadening.

The $1 + Q + Q^{-1}$ dependence of h in Eq. (13) gives the well-known van Deemter plot [39]. In the working range of linear velocity used in our preparative experiments, the γ's are negligible and Eq. (13) can be simplified to a linear relation between h and Q, because Pe is

roughly constant and the α's are only weakly dependent on Q. For computational convenience, however, the γ's are assigned a small, but realistic value, in order to keep the boundary condition in Eq. (11) valid when $Q = 0$, i.e., when the flow through a column is halted.

4.2. Dynamic process model

The GSSR process's model is obtained by assembling N instances of the chromatographic column model, one for each of the N columns, and linking them through appropriate material balances written for the inlet nodes of the columns.

The node balances at each column inlet are written in a way that mimics our experimental implementation of the GSSR process. Binary variables (i.e., variables that can only take the values 0 or 1) are introduced to define the state of the two-way valves installed in the pilot unit (Fig. 3); if the variable is equal to 0, the valve is closed; if it is equal to 1, the valve is open.

The material balances on the flow rates at the N column inlets are

$$Q_1 = (1 - \upsilon_N^{\mathrm{W}} - \upsilon^{\mathrm{P}})Q_N + \sum_{s \in \mathcal{S}} \upsilon_1^s Q_s + \upsilon^F Q_{\mathrm{F}}, \tag{15}$$

$$Q_j = (1 - \upsilon_{j-1}^{W})Q_{j-1} + \sum_{s \in \mathcal{S}} \upsilon_j^s Q_s \quad (j = 2, \ldots, N), \tag{16}$$

where $\mathcal{S} = \{\mathrm{A}, \ldots, \mathrm{D}\}$ represents the train of solvents; the υ's, the states of the corresponding two-way valves depicted in Fig. 3; Q_j, the volumetric flow rate through column j; Q_s, the flow rate of solvent s; and Q_{F}, the feed flow rate. We recall that for our pilot unit, $N = 3$.

The balance for column 1 is different from the other two balances, because its inlet is connected to the feed line, and because the outlet of its upstream neighboring column (i.e., column 3) is connected to the product line. Note also that Eq. (15) is written under the assumption that υ_N^{W} and υ^{P} are never both set to 1 at the same time, because it is physically impossible to simultaneously collect waste and product from the same column outlet. To obtain a more robust mathematical balance, it suffices to replace $(1 - \upsilon_N^{\mathrm{W}} - \upsilon^{\mathrm{P}})$ by $(1 - \max\{\upsilon_N^{\mathrm{W}}, \upsilon^{\mathrm{P}}\})$.

The component material balances at the column inlets can be written a

$$(Qc_i^{\mathrm{in}})_1 = (1 - \upsilon_N^{\mathrm{W}} - \upsilon^{\mathrm{P}})(Qc_i^{\mathrm{out}})_N + \sum_{s \in \mathcal{S}} \upsilon_1^s Q_s c_i^s + \upsilon^F Q_{\mathrm{F}} c_i^{\mathrm{F}}, \tag{17}$$

$$(Qc_i^{\mathrm{in}})_j = (1 - \upsilon_{j-1}^{W})(Qc_i^{\mathrm{out}})_{j-1} + \sum_{s \in \mathcal{S}} \upsilon_j^s Q_s c_i^s \quad (j = 2, 3), \tag{18}$$

where c_{ij}^{in} and c_{ij}^{out} are the concentrations of component i at the upstream and downstream ends of column j, respectively; c_i^s is the concentration in solvent s; and c_i^{F} is the concentration in the feed.

Note that in Eqs. (17) and (18), i runs over the set of solutes and the solvent modifier ($i = 0$). Obviously, $c_i^s = 0$ for $i > 0$ and $s \in \{\mathrm{A}, \ldots, \mathrm{D}\}$ because the peptide mixture is not injected into the system via the train of solvents. The c_i^{F}, on the other hand, are different from zero for $i > 0$, because they define the feedstock composition; moreover, c_0^{F} defines the modifier concentration in the feed. The concentrations c_0^s for $s \in \{\mathrm{B}, \ldots, \mathrm{D}\}$ are constant (i.e., time independent), because they define the modifier concentrations in the isocratic solvents; but the modifier concentration, c_0^{A}, in the solvent-gradient line, A, is time variable according to piecewise-linear periodic profile given by Eq. (1).

4.3. Numerical solution

The GSSR's dynamic process model was solved using two different numerical solution strategies. In one case the model equations were solved directly for cyclic steady state (CSS) conditions to get the GSSR's steady periodic solution. To this end, each instance of the chromatographic column model—one for each column—was discretized both in time, $t \in [0, N\tau]$, and in the spatial coordinate, $z \in [0, 1]$, and the GSSR's CSS condition

$$c_{ij}(t + N\tau, z) = c_{ij}(t, z) \quad \forall z \in [0, 1] \tag{19}$$

was directly applied at $t = 0$ [this gives $c_{ij}(N\tau, z) = c_{ij}(0, z)$]. This full-discretization approach gives rise to a large sparse system of nonlinear equations that can be solved using a suitable solver.

Note that the GSSR's CSS condition is different from the CSS condition for multi-column, simulated counter-current adsorption processes [41–44]:

$$c_{i,j+1}(t + \tau, z) = c_{ij}(t, z). \tag{20}$$

This is because the GSSR's feed inlet and product outlet lines are attached to fixed columns and, therefore, do not advance their position by one column at the end of every switching interval as all other lines do.

The method above provides the steady periodic solution, but not the initial transient cycles until the CSS is attained, starting, e.g., from a clean system, nor the path followed by the process between two steady periodic states because of a change in an operating parameter. To determine the GSSR's cycle-to-cycle dynamics we employed a standard method-of-lines approach: the model was discretized in the spatial coordinate, $z \in [0, 1]$, to obtain a sparse system of differential-algebraic equations (DAE) for which robust and computationally efficient software is widely available to generate a numerical solution along the time coordinate.

5. Results and discussion

5.1. Adsorption equilibria

When dealing with the purification of a complex, multicomponent mixture, like the crude peptide mixture, it is convenient to minimize the number of solutes taken into consideration in the design procedure to make it numerically tractable. This is similar to the method often used in dealing with the design of distillation columns for the separation of petroleum fractions, where only a few selected key components are considered in the calculations. In the present case, five key components were selected: the most weakly adsorbed (earliest eluting) impurity ($i = 1$), the target product ($i = 3$) and its two closest impurities ($i = 2$ and $i = 4$), and the most strongly adsorbed (latest eluting) impurity ($i = 5$). The key components are identified by arrows pointing to their elution peaks in the analytical chromatogram of Fig. 4.

To determine the influence of the EtOH concentration, c_0, on the adsorption behavior of the peptide mixture, 250 μL pulses of the crude mixture at 1 g/L were injected into the analytical Kromasil column and eluted isocratically for various values of c_0; the flow rates in these experiments were in the range 0.3–0.6 mL/min (data not shown).

From the experimental chromatograms it is easy to determine the retention times of the key components for each value of c_0. The retention time, t_i, for solute i, is related to the thermodynamic and elution parameters by

$$t_i = \frac{\epsilon + K_i}{Q/V}. \tag{21}$$

From the known value of t_i it is straightforward to determine the Henry's constant, K_i, or, more conveniently, the value of $\epsilon + K_i$:

$$\epsilon + K_i = \frac{t_i Q}{V}. \tag{22}$$

Table 1
Values of $\epsilon + K_i$ for the key components of the peptide mixture, as a function EtOH concentration, c_0 (% (v/v)), and their fitting to an expression of the form $K_i = K_i'/(c_0/100)^{n_i}$; data calculated from the retention times using Eq. (22).

c_0 (% (v/v))	Key component				
	1	2	3	4	5
$\epsilon + K_i$					
20	1.25	8.02	10.47	12.47	21.63
25	0.61	3.85	4.87	5.79	9.13
30	0.62	2.35	2.72	3.14	4.54
40	0.61	1.20	1.29	1.42	1.73
50	0.59	0.82	0.85	0.89	0.95
K_i'	8×10^{-7}	0.016	0.016	0.018	0.017
n_i	8.36	3.83	4.02	4.08	4.47

The calculated values of $\epsilon + K_i$ are listed in Table 1, where it is shown that for the least retained component, $\epsilon + K_1$ stabilizes at ≈0.61 as c_0 is increased. Since the value of $\epsilon[=\epsilon_b + (1-\epsilon_b)\epsilon_p]$ for a well-packed column chromatographic column is usually in the range 0.60–0.70, we take $\epsilon = 0.61$ and assume that for practical purposes the least retained solute does not adsorb for large values of c_0; this allows us to calculate the values of K_i $[=(1-\epsilon_b)H_i]$ for all the key components.

The dependence of each K_i on c_0 was fitted to a function of the type $K_i = K_i'/c_0^{n_i}$, which is identical to the one used in the development of Eq. (10); the fitted values of K_i' and n_i are listed in the two bottom lines of Table 1. The fitted curves are directly compared with the experimental data in Fig. 5, which shows that the dependence of K_i on c_0 is well described by an equation of the form $K_i = K_i'/c_0^{n_i}$.

To stress the difficulty of the peptide separation problem, the Henry constant of the target peptide ($i=3$) and those of its two closest impurities ($i=2$ and $i=4$) are plotted against c_0 in Fig. 6 for comparison. When the K-curves are plotted together and compared, it is seen that the retention factors of the two impurities are very close to that of the target peptide. This makes the purification of the target peptide a difficult separation problem and, thus, a good case study for the GSSR process. Note also that the selectivities, $\alpha_{ij} = K_j/K_i = (H_j/H_i)c_0^{n_i - n_j}$, for the pair combinations (i, j) of the three solutes are weakly dependent on c_0 because $n_i - n_j \approx 0$. Thus, the solvent gradient must be properly placed along the three columns to effectively help at accomplishing the separation.

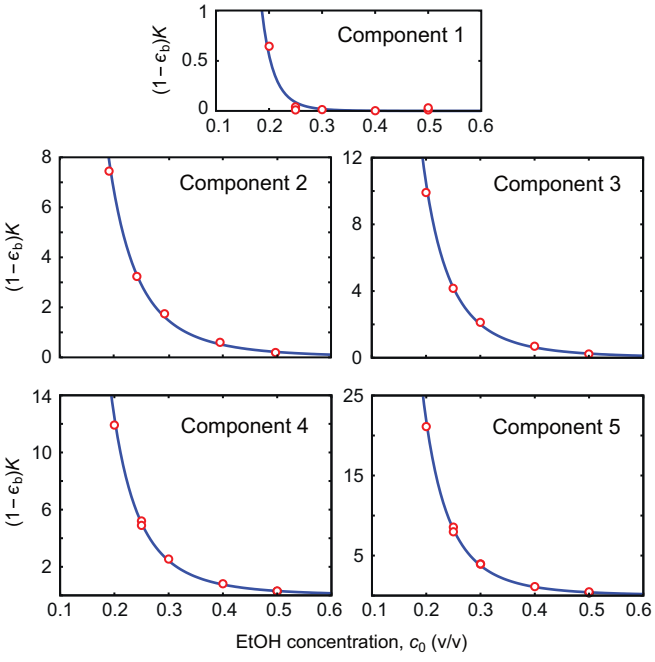

Fig. 5. Henry constants, $K_i = (1-\epsilon_b)H_i$, for the key components of the peptide mixture, as a function of EtOH concentration, c_0 (v/v). Symbols are experimental data and lines are plots of $K_i'/c_0^{n_i}$ with parameters taken from Table 1.

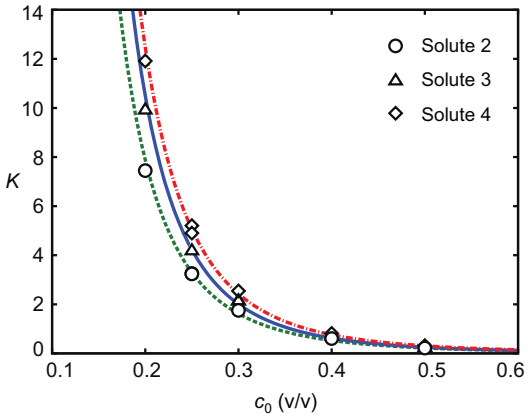

Fig. 6. Henry constants, $K_i = (1-\epsilon_b)H_i$, for the target peptide ($i=2$) and its two closest impurities ($i=2$ and $i=3$), as a function of EtOH concentration, c_0 (v/v). Symbols are experimental data and lines are plots of $K_i'/c_0^{n_i}$ with parameters taken from Table 1.

5.2. Validation of moving solvent-gradient in the pilot unit

Before applying the GSSR process to the purification of the crude peptide mixture, the pilot unit underwent extensive testing in order to validate the automation of the valve sequencing, pump actuation, solvent-gradient implementation by the admixture of two isocratic pumps, pulsed feeding, and waste and product collecting. For example, some preliminary tests to validate the automation of the pumps and valves was carried out on the pilot unit using pure water and without the three chromatographic columns, which were simply replaced by capillary tee connections. The rate of accumulated mass from the waste and product lines was monitored in real time using a precision balance, model TE3102S from Sartorius (Goettingen, Germany). The rate of accumulated mass, dm/dt (g/min), is proportional to the flow rate, Q (cm^3/min), the scaling factor being the density ρ (g/cm^3) of the fluid: $\rho^{-1}(dm/dt) = Q$. The balance reading gives the mass accumulated over a given period of time, $m = \rho \int Q\,dt$. Although these tests were very successful (data not shown), they gave only a partial, and necessarily limited, validation of the practical implementation of the GSSR cycle on the pilot unit.

More realistic tests on the implementation of the moving solvent-gradient were performed on the pilot unit with three columns and a nonadsorbed tracer. The three chromatographic columns employed in these tests are Superformance 26-mm ID thermo-jacketed glass columns (Götec Labortechnik, Mühltal, Germany). Reversed-phase Source 30 RPC (30 μm particle size; GE Healthcare Amersham Biosciences, Uppsala, Sweden) was slurry packed into each column to a bed height of $L = 6$ cm with 5% (v/v) ethanol/water at 25 mL/min, back-pressure of 30 bar, and 30 min packing time.

In these tests, changes in the solvent composition (say, changes in the water/ethanol ratio) were replaced by equivalent changes in the concentration of blue dextran (BD) in an isocratic solvent. BD is a dextran polymer with an average molecule weight of 2×10^6. Its large molecular size prevents it from penetrating into the pore volume of the adsorbent particles; in practice, this tracer probes the interparticle void volume in the columns and extra-column dead volumes.

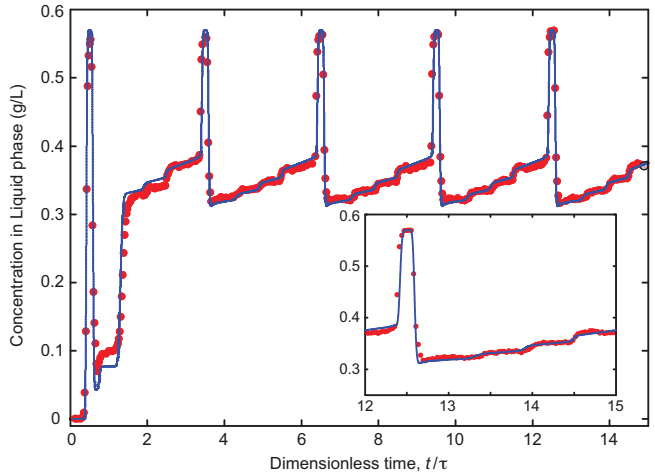

Fig. 7. Temporal profile of blue dextran concentration at the outlet of column 3 for 5 cycles of a GSSR process. Lines are the theoretical predictions and symbols are the experimental UV data. The inset at lower-right zooms the profile for the 5th cycle.

Fig. 7 compares the BD's concentration profile measured by UV at the outlet of column 3 with the profile predicted by process simulation. In this tested GSSR cycle, feed is introduced into column 1 and product collected from column 3. The switching interval is $\tau = 5$ min and the feed (pure water) flow rate, $Q_F = 0.5$ mL/min. The duration of the desorption zone is $\Delta t_D/\tau = 0.25$; the instants, scaled by the cycle time, when feed is injected an the product is collected are the same and equal to $t_F/\tau_{cyc} = t_P/\tau_{cyc} = 0.667$ (beginning of the third switching interval); the duration of the feed pulse is $\Delta t_F = 30$ s and the duration of the product withdrawal is $\Delta t_P = 60$ s. The compositions and flow rates of the solvent lines are: solvent A1, 0.24 g/L, solvent A2, 0.44 g/L; $Q_{A1} + Q_{A2} = 5$ mL/min; solvent B, 0.25 g/L, $Q_B = 1$ mL/min; solvent C, 0.25 g/L, $Q_C = 1.25$ gL/min; and solvent D, 0.57 g/L, $Q_D = 5$ mL/min.

The theoretical profile shown in Fig.7 was predicted by the GSSR model with interparticle porosity $\epsilon = 0.39$, intraparticle porosity $\epsilon_p = 0$, and Péclet number $\mathrm{Pe} = vL/D_L = 700$, where v is the linear velocity of the fluid and D_L is the dispersion coefficient. The GSSR model was solved for $n_c = 0$, since the solvent ($i = 0$) is the only component in the system. (The default values $H'_0 = 0$ and $n_0 = 0$ guarantee that it does not adsorb.) The effect of dead volumes in the pilot unit was lumped into the value of ϵ; extra-column volumes represent roughly $100 \times (0.39 - 0.32) = 7\%$ of the volume of the packed beds. Fig. 7 shows that there is good agreement between the experimental profile and the theoretical one. We can now tackle more confidently the difficult center-cut purification problem of the crude peptide mixture.

5.3. GSSR cycle for purification of the peptide mixture

The GSSR cycle for the purification of the crude peptide mixture consists of a standard cycle with a desorption step ($\Delta t_D > 0$), in which the feed and production steps start at the beginning of the third switching interval ($t_F = t_P = 2\tau$); this cycle is quite similar to the one tested with the blue dextran tracer.

5.3.1. Shortcut design procedure

The design procedure for a chromatographic process should not be too complicated or tedious, nor should it be time consuming, otherwise the process will be of limited use in industrial practice. Here, we briefly describe a simple shortcut procedure for designing a GSSR cycle, which is based only on the retention times of the key components.

The EtOH concentration in the solvents is restricted to the range 25–50% (v/v); over this working range, the values of $\epsilon + K$ for the target peptide and its two closest impurities decrease by roughly 80%, thus giving a good extent of variation of the retention times. For simplicity, the EtOH concentrations in solvents B and C are fixed at 25% (v/v) and that in the stronger solvent D at 50% (v/v). The gradient is applied somewhere in between these two values. The train of solvents is handled with only two solvent storage tanks: one with 25% (v/v) EtOH and the other with 50%. The solvent gradient (solvent line A) is built from the admixture of different amounts of solvent drawn from the two tanks.

Given that the HPLC pumps have 10 mL heads, we design the system with external flow rates of roughly 1–5 mL/min and a maximum internal flow rate around 8 mL/min, which for the GSSR cycle is given by $Q_A + Q_B + Q_C$. Solvent A is responsible for doing most of the separation, whereas the purpose of solvents B and C is to restrain the width of the central cut by adding a little more retention to the side parts of the target peak that are recycled. The mixed cut with the leading edge of the target peptide is diluted with solvent C during recycling (step d of Fig. 1), whereas the mixed cut with the trailing edge is diluted with solvent B (step f of Fig. 1). Thus solvent C should have a somewhat higher flow rate than solvent B, because the leading mixed cut is less retentive than the trailing one. If the flow rates of the isocratic solvents are fixed at $Q_B = 1$ mL/min and $Q_C = 1.25$ mL/min, the flow rate of the solvent gradient should be $Q_A \approx 5.7$ mL/min to give a maximum internal flow rate of 8 mL/min.

The cycle time is fixed at ca. 10 min; this gives $\tau = 3 + 1/3$ min, which we round up to 3.5 min. We want the central cut to move from one column to the next over the duration of a switching interval by the injection of the solvent gradient. To achieve this, the retention time of the target solute in one column should be equal to the switching interval, i.e.,

$$[\epsilon + K_3(\bar{c}_0)]V + V_e = Q_A\tau. \tag{23}$$

Here, V is the column volume; V_e is the extra dead volume per column; K_3 is the Henry constant of the target peak; and $\bar{c}_0$, the EtOH concentration at which the gradient is centered around. Solving for $\bar{c}_0$ gives 34.0% (v/v). Thus, working with 34% (v/v) EtOH in the solvent will induce a retention time of the target peptide per column equal to the switching interval. By applying the same procedure to the two closest impurities, gives 32.4% (v/v) for the less retained one and 35.4% for the more retained. So as a first approximation, a total gradient from 32.4% to 35.4% (v/v) is to be expected.

Complete elution of the most retained impurity at 5 mL/min with solvent D (50% (v/v) EtOH) gives $\Delta t_D \approx 1.5$ min. The feedstock is diluted in 25% (v/v) EtOH solvent at $c^F = 0.53$ g/L, and 1 mL of feed solution is injected per cycle, which gives a feed pulse of $\Delta t_F = 0.5$ min at $Q_F = 2$ mL/min. This feed concentration is in the linear response range of the UV detector, well below its saturation limit. The width of the central cut, as measured by the positions of the two closest impurities, is about 1/3 of a column length; using an expression similar to Eq. (23), but with its l.-h.-s. multiplied by 0.33 and τ replaced by Δt_P, gives a collection time of about 1.1 min that we round down to $\Delta t_P = 1$ min in order to introduce a small safety margin.

The set of operating parameters are summarized in Table 2 and were found to be adequate for exploratory experiments with the GSSR pilot unit.

5.3.2. Step sequencing

To determine the sequencing of the inlet/outlet lines for the selected GSSR cycle, we resort to the schematics in Figs. 1 and 2. During the first two switching intervals of the cycle the train of solvents is unaffected by the feed and production steps, because these steps occur during the third switching interval. Thus, the chrono-

Table 2
Operating parameters of the GSSR cycle. Second and third columns give, respectively, the EtOH concentration, c_0, and the flow rate of the solvent line; solvent-gradient A increases c_0 linearly from 32.4% to 35.4% (v/v) over every switching interval. Notation: τ, switching interval; t_F and Δt_F, position and duration of feed injection; t_P and Δt_P, position and duration of product collection; Δt_D, duration of desorption step.

	(% (v/v))	(mL/min)		(min)
Feed	0.25	2.0	τ	3.5
Solvent A	0.324–0.354	5.7	Δt_D	1.5
Solvent B	0.25	1.0	Δt_F	0.5
Solvent C	0.25	1.25	Δt_P	1.0
Solvent D	0.50	5.0	t_F, t_P	7.0

grams of port switching for the first two switching intervals of the cycle are taken directly from steps a to d in Fig. 1.

The feed and production steps start at the beginning of the third switching interval, but it must be noted that the production step is longer than the feed step ($\Delta t_P > \Delta t_F$); moreover, both steps occur while the desorption step is performed on the third column, because $\Delta t_D > \max(\Delta t_F, \Delta t_P)$. Thus, the third switching interval starts with the two bottom steps of Fig. 2; the duration of the first step is Δt_F and that of the second is $\Delta t_P - \Delta t_F$. Finally, the cycle ends with the sequencing of the solvent lines given by steps *e* and *f* of Fig. 1; but note that step *e* takes $\Delta t_D - \Delta t_P$ and is followed by step *f* for the remaining $\tau - \Delta t_D$ of the switching interval.

5.3.3. Simulated cycle

The full GSSR cycle is shown in Fig. 8, along with snapshots of the simulated axial concentration profiles in the three columns taken at selected instants of the cycle when switching between some of the steps. For a better visualization, the concentration profiles have been scaled by the corresponding concentrations in the feed; this has the effect of magnifying the profiles for the impurities, which would, otherwise, be difficult to discern for some steps of the cycle. The axial solvent composition profile is represented by the dashed lines on a secondary *y*-axis with a linear scale ranging from 25% to 50% (v/v) EtOH. The duration of each step of the cycle is given at the left of the corresponding flow diagram; thus the first step takes Δt_D time units, the second step takes $\tau - \Delta t_D$ time units, and so forth.

Fresh feedstock fluid is injected into the upstream end of column 1 at the start of the third switching interval, while at the same time the target peptide contained in the feed pulse injected in the previous cycle is obtained in purified form at the downstream end of column 3. This way, each pulse of feed injected per cycle is forced to travel over the entire length of the system to get maximum separation between neighbor peaks.

Product withdrawal starts after the recycle of solute 2 and of the cut in which it is mixed with the leading edge of the product. The product collecting step continues until breakthrough of the target peptide's slower neighbor impurity. After product collection, the impure cut containing the trailing edge of the target peptide mixed with its slower neighbor impurity is recycled to the upstream end of column 1. Ideally, this cut should be injected into the upstream end of column 1 right after the injection of feed. To achieve this, and since the product collecting step is longer than the feed step, the feed column (i.e., column 1) is frozen during the last $\Delta t_P - \Delta t_F$ time units of product collection to wait for the recycled cut.

The more weakly adsorbed impurity is pushed into column 2 during the third switching interval and then purged out of the system during the first switching interval of the following cycle. The most weakly adsorbed impurity is taken out of the system through column 2 during the last step of the cycle and the first step of the following cycle (these two steps are contiguous in time). The most strongly adsorbed impurity, which is the slowest traveling species in the system, is purged out of the system mostly during the strong desorption step applied to column 2, but with a delay of one cycle. The product's slower neighbor impurity is discarded from the system in three waste cuts taken from the three columns; the product's faster neighbor impurity is taken out of the system through columns 2 and 3.

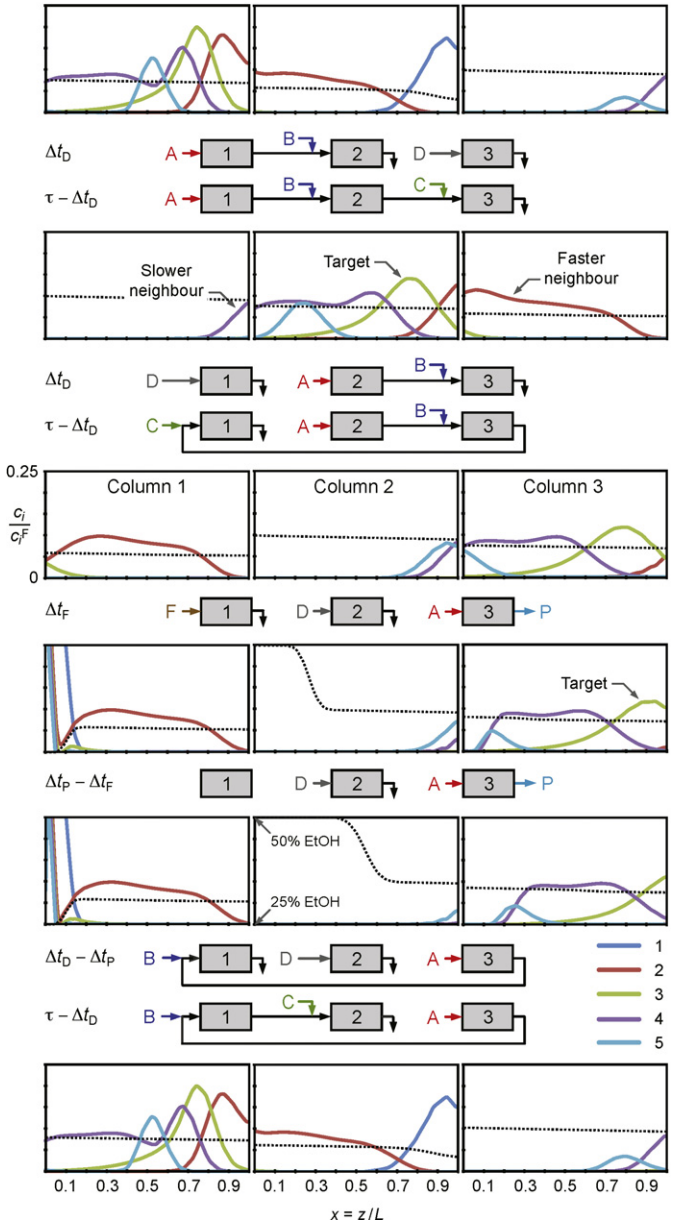

Fig. 8. GSSR cycle for purification of the peptide mixture and snapshots of the simulated axial concentration profiles taken at selected instants of the cycle. The dashed lines represent the EtOH axial concentration profiles (v/v). The operating parameters are listed in Table 2.

5.4. Choice of manipulated variable for tuning the process

Whatever procedure is employed for process design, even a computer-aided one based on a detailed process model, it is always necessary to dynamically adjust some of the operating parameters during process operation to compensate for deviations from the target purity arising from imperfect design and experimental variability.

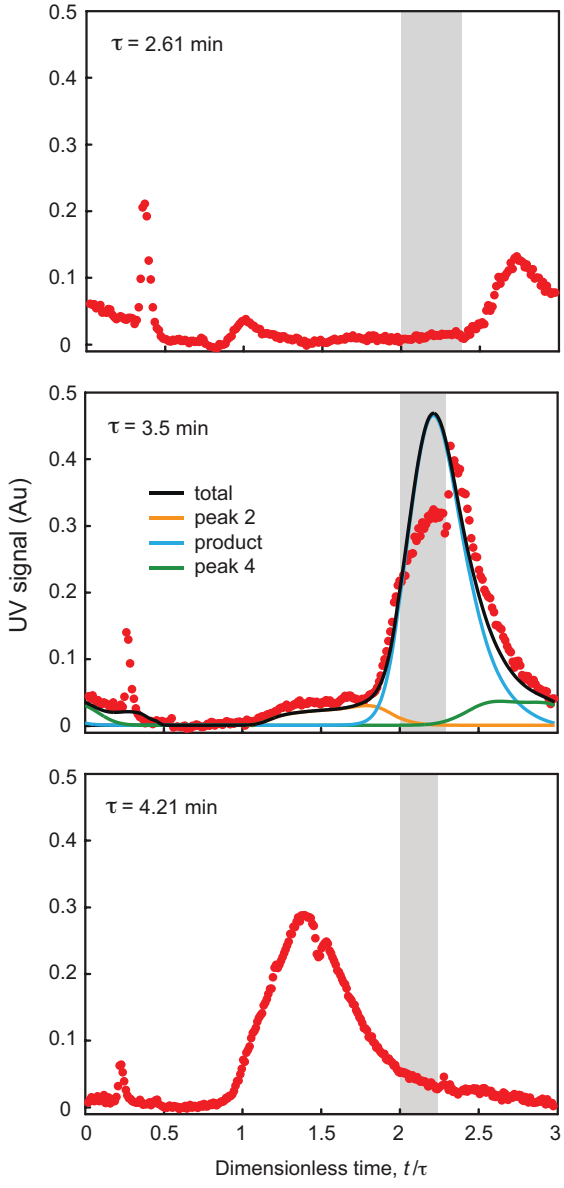

Fig. 9. Effect of the switching interval, τ, on the elution time of the main product peak at the outlet of the column where the product fraction is collected. The experiment started with $\tau = 3$ min and then its value was changed every three cycles to one of the values shown in the graphics; the sequence was from top to bottom. Each graph shows the experimental UV profile at the column outlet before changing the value of τ. The gray area shows the time interval for product collection. The lines for $\tau = 3.5$ min are the simulated concentration profiles of the central key components of the peptide mixture (the product and its two nearest impurities); the black line is the simulated total concentration profile.

The switching interval, τ, was selected as manipulated variable for dynamically adjusting the GSSR process. The efficacy of this choice was verified by a parametric and sensitivity analysis of the process using the model-based tools described above, and is in line with methods proposed by some authors for controlling the SMB process [45].

Fig. 9 shows an experimental study of the effect of τ on the UV signal at the outlet of column 3—the one from which product is collected—over a full GSSR cycle. The purified product cut is clearly identified by a broad peak in the UV signal. For $\tau = 2.61$ min the purified product exits column 3 after the collection has taken place, whereas for $\tau = 4.21$ min the purified cut exits column 3 before being diverted for product collection; for $\tau = 3.5$ min, the product peak seems to be well positioned with respect to the collecting interval, as can be seen by the simulated composition profiles which have been superposed on the experimental graphic.

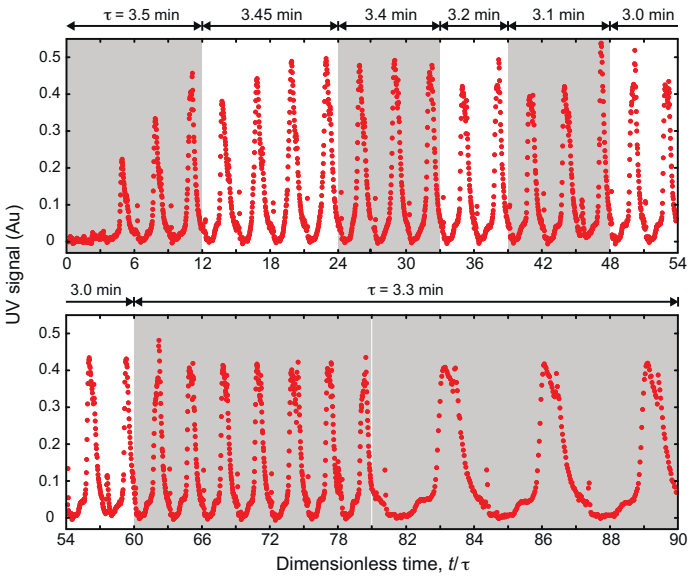

Fig. 10. Temporal profile of the UV signal measured at the outlet of column 3 for the 30-cycle GSSR experiment.

5.5. Experimental GSSR run

As an experimental proof of concept of the GSSR process, the pilot unit was operated over a long period of time—30 full cycles—in order to attain the cyclic steady state conditions and to assess the reproducibility and stability of the pilot unit over a long period of operation. Fig. 10 shows the temporal UV profile at the outlet of the third column for the 30-cycle GSSR experiment; in this figure the time scale is made dimensionless by dividing the process time by the value of the switching interval, τ; with this time scaling, a complete GSSR cycle takes three dimensionless time units, and the cycles start at $t/\tau = 0, 3, 6, 9$, and so forth.

As discussed above, τ was employed as a manipulated variable to adjust the relative position of the moving composition profile in the GSSR loop with respect to the outlet ports. The switching interval was initially set at $\tau = 3.5$ min. However, while monitoring the UV signal at the outlet of the third column, and using as a guide the position of the product peak with respect to the time frame for product collecting, the value of τ was ultimately decreased to 3.3 min; this action corrected the relative position of the moving composition profile in the GSSR loop.

The value of τ for each cycle is shown at the top of Fig. 10. The value of τ was initially set to 3.5 min over the first 4 cycles, but was then adjusted to 3.45 min over the following 4 cycles in an attempt to move the collected product fraction to the correct position. Based on the elution time of the product peak at the outlet of column 3, the initial reduction of τ to 3.45 min was found to be insufficient, so its value was further reduced to 3.4 min over the following 3 cycles, then changed to 3.2 min over another 3 cycles, further reduced to 3.1 min for another 3 cycles, and finally settled at 3.0 min for another 4 cycles. The elution times of the main product peak at the outlet of column 3 for values of τ equal to 3.0, 3.1, 3.2 and 3.4 min were fitted to a third-order polynomial, from which the optimum value of τ was determined to be $\approx$3.3 min. This value of τ was kept fixed over the last 16 cycles of operation.

Fig. 11 shows the temporal UV profile at the outlet of column 3 for the last four cycles of the 30-cycle GSSR run, i.e., cycles 27

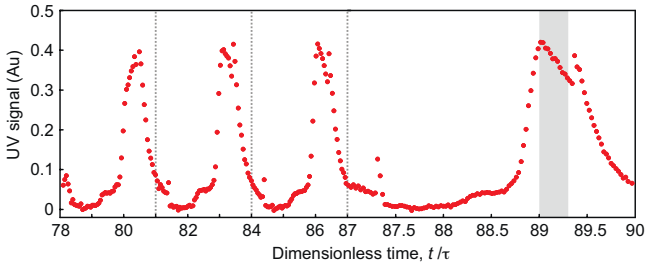

Fig. 11. Temporal profile of the UV signal measured at the outlet of column 3 for the last four cycles of the 30-cycle GSSR experiment. The time scale for the 30th cycle is expanded to improve visual clarity. The grayed area shows the time interval during which product was collected in the 30th cycle.

through 30. The time coordinate is scaled by the value of the switching interval and expanded for the 30th cycle for better visualization. The grayed rectangle shows the interval during which product is collected in the last cycle of the run; the peak in the UV signal appears to be well positioned by reference to Fig. 9.

Fig. 12 shows the HPLC analysis of the product fraction collected over the 30th cycle; the analytical chromatogram of the product cut demonstrates that the product purity obtained experimentally meets the value originally aimed at, i.e., $pur_p \geq 98\%$. Actually, it is visually difficult to discern the existence of any trace of the faster neighbor impurity in the chromatogram of Fig. 12; however, our peak fitting procedure detects a small amount of impurity within the scatter of the UV signal's baseline, which is why we do not report 100% purity for the collected product fraction.

Purity is not the only determining performance variable for the chromatographic separation of a high value-added bioproduct; recovery is also another important performance variable. The product recovery for the experimental GSSR run was determined by the following procedure. The concentration of the target peptide in the product fraction, c_p^P, can be determined by comparing the peak areas for the target peptide in two analytical chromatograms: one for the feed (top graph of Fig. 4) and the other for the collected product fraction (Fig. 12). Since the volumes of injected sample were the same in both chromatograms,

$$c_p^P = \frac{A_p^P}{A_p^F}\frac{Q^F}{Q^P}c_p^F, \tag{24}$$

where c_p^F is the solute concentration in the feed mixture, A_p^F is the peak area of the target solute in the analytical chromatogram of the feed mixture (Fig. 4), and Q^F is the flow rate at which the chromatogram was obtained; A_p^P is the peak area of the target peptide in the chromatogram of the product fraction from the GSSR process (Fig. 12) and Q^P is the flow rate at which the corresponding chromatogram was obtained. In the present case, the values are $Q^F = 0.558$ mL/min, $Q^P = 0.631$ mL/min, $A_p^F = 0.769$ mAU×min, $A_p^P = 0.1145$ mAU×min, and $c^F = 0.5295$ g/L. From Eq. (24), we get $c^P = 0.089$ g/L. The amount of target solute injected per GSSR cycle is $f_p = c_p^F Q_F \Delta t_F = (0.5295\ \text{g/L})(2\ \text{mL/min})(0.5\ \text{min}) = 0.529$ g and the amount of target solute collected per cycle in the purified cut is $m_p = c_p^P Q_P \Delta t_P = (0.089\ \text{g/L})(5.7\ \text{mL/min})(1\ \text{min}) = 0.505$ g (note that for the GSSR cycle under analysis, $Q_P = Q_A$); therefore, the product recovery is $rec_p = m_p/f_p = 0.505/0.529 = 95.3\%$.

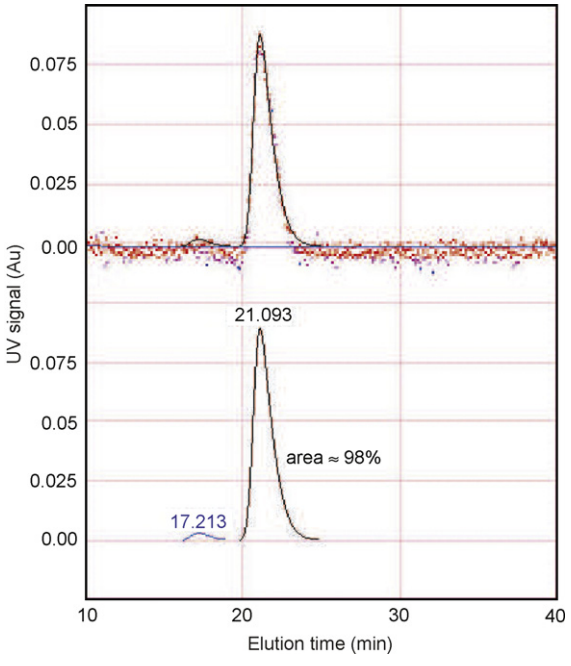

Fig. 12. HPLC analysis of the product fraction collected during the last cycle of the 30-cycle GSSR experiment of Fig. 10.

5.6. Comparison with single-column batch chromatography

We have determined by simulation the optimal operation of single-column batch chromatography with linear solvent gradient, and compared its performance with that of the 30-cycle GSSR experiment for the same amount of stationary phase and same amount of feed injected per cycle. The best solvent-gradient policy for the batch process that maximizes the recovery of the target peptide for purity specifications above 90% turns out to be isocratic elution. To see why this is so, first notice that the Henry constants given in Table 1 decrease monotonically with the EtOH concentration (c_0) in the solvent. But more importantly, however, is that the selectivities between the target peptide and its two neighbor impurities, α_{21} and α_{32}, where

$$\alpha_{ij} = \frac{1+\beta K_i}{1+\beta K_j} \tag{25}$$

and $\beta = (1-\epsilon)/\epsilon$ is the phase ratio, also follow the same trend with respect to c_0. Since the batch process does not achieve baseline separation of the target product from its two neighbor impurities at the lowest EtOH concentration considered in the GSSR experiments ($c_{0,\min} = 0.25$ (v/v)), the three peaks will elute even closer to each other if the value of c_0 is increased. Thus, the optimal solvent-gradient policy for the batch process that maximizes the recovery is isocratic elution with $c_0 = c_{0,\min}$.

Fig. 13 shows the numerical results of maximizing the recovery, rec_p, achieved by the batch process for purity specifications $pur_p \geq (pur_p)_{\min}$ in the range $0.9 \leq (pur_p)_{\min} \leq 0.98$. The amounts of stationary phase and feed injected per cycle are the same as those for the 30-cycle GSSR experiment. Fig. 13 shows that the GSSR process performs considerably better than the batch process: in the experimental GSSR run 95.3% of the target product was recovered with 98% purity, whereas only 52% of the product would be recovered at the same purity with the batch process.

Since there is a single outlet in a one-column system, it is not possible to reject waste fractions—e.g., one containing the most weakly retained impurities—early in the cycle through intermediate waste outlets as in a multicolumn system. This imposes a constraint on the minimum length of the cycle for the batch process, which has a direct impact on its productivity. The GSSR process, on the other hand, is not limited by this constraint. As a result, the productivity achieved in the 30-cycle GSSR experiment is 4.2 times higher than the productivity that would be achieved with the batch process for the same purity specification of 98%.

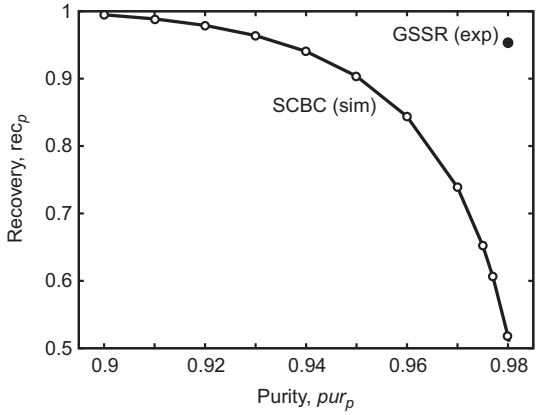

Fig. 13. Simulated curve of optimal product recovery (rec_p) versus purity (pur_p) for single-column batch chromatography (SCBC) subject to the same amount of stationary phase and amount of feed injected per cycle as in the 30-cycle GSSR experiment. The open circles are the optimal numerical solutions of the maximization of rec_p for the batch process subject to the purity constraint $pur_p \geq (pur_p)_{min}$, for various values of $(pur_p)_{min}$; the closed circle gives the performance of the experimental GSSR run.

6. Conclusions

A new multicolumn, open-loop process for center-cut separation by solvent-gradient chromatography has been introduced. The process combines the simulated counter-current operation of a moving solvent gradient with steps of pulsed feed injection and product withdrawal at fixed positions in a train of columns. With the use of multiple columns, better solvent gradients can be implemented and the cuts can be manipulated more flexibly. Moreover, by means of the port switching it is possible to recycle some of the mixed cuts from the downstream end of the system to its upstream end, thereby increasing product recovery. We have shown that this can be done while working in a simple, open-loop system that resembles the batch system.

The experimental results presented here show that the GSSR process can separate an intermediate retained component from complex mixtures of biomolecules with nearby-eluting impurities, with high purity without sacrificing the product recovery. The GSSR experiments reported here were performed under diluted, linear conditions, which necessarily limits the assessment of the process performance to purity and recovery. For example, it is difficult to report on specific productivity and solvent consumption for a linear system; under those conditions, one cannot discuss about absolute values and the best we can do is to compare productivity and solvent consumption between processes for the same amount of stationary phase. For example, if the value of $Q_F \Delta t_F rec_p/\tau_{cyc}$ is higher for process *x* than for process *y*, then the productivity of process *x* is higher than that of process *y*, and a similar reasoning can be applied to the solvent consumption; we have followed this procedure above to compare the performance of the GSSR process and that of the batch process.

The GSSR process also appears to be easy to control, as we have demonstrated by dynamically adjusting the value of the switching interval to correct the position of the moving composition profile in the GSSR loop with respect to the outlet ports. Upcoming research will provide further demonstrations that the GSSR process can perform difficult separations better and more efficiently than the current batch gradient process, and will compare its performance against those of other competing processes under conditions not limited by the feed concentration.

Acknowledgements

R. Silva, R. Rodrigues, and J. Mota acknowledge funding from FCT/MCTES (Portugal) through grants SFRH/BD/48054/2008, SFRH/BPD/48366/2008, and PTDC/EBB-BIO/101992/2008.

References

[1] G. Walsh, Trends Biotechnol. 23 (2005) 553.
[2] A.C.A. Roque, C.R. Lowe, M.A. Taipa, Biotechnol. Prog. 3 (2004) 639.
[3] R. Wooley, Z. Ma, N.-H.L. Wang, Ind. Eng. Chem. Res. 37 (1998) 3699.
[4] P. Wankat, Ind. Eng. Chem. Res. 40 (2001) 6185.
[5] A. Nicolaos, L. Muhr, P. Gotteland, R.M. Nicoud, M. Bailly, J. Chromatogr. A 908 (2001) 71.
[6] A. Nicolaos, L. Muhr, P. Gotteland, R.M. Nicoud, M. Bailly, J. Chromatogr. A 908 (2001) 87.
[7] A.S.T. Chiang, AIChE J. 44 (1998) 1930.
[8] Y.A. Beste, W. Arlt, Chem. Eng. Technol. 25 (2002) 956.
[9] J.K. Kim, Y. Zang, P.C. Wankat, Ind. Eng. Chem. Res. 42 (2004) 4849.
[10] S. Abel, M.U. Babler, C. Arpagaus, M. Mazzotti, J. Stadler, J. Chromatogr. A 1043 (2004) 201.
[11] G. Paraedes, S. Abel, M.U. Babler, M. Mazzotti, M. Morbidelli, J. Stadler, Ind. Eng. Chem. Res. 43 (2004) 6157.
[12] W. Jin, P.C. Wankat, Ind. Eng. Chem. Res. 44 (2005) 1565.
[13] W. Jin, P.C. Wankat, Ind. Eng. Chem. Res. 45 (2006) 2793.
[14] E. Valéry, O. Ludemann-Hombourger, World Patent WO 2007/012750 A2, 2007.
[15] R.C.R. Rodrigues, T.J.S.B. Canhoto, J.M.M. Araújo, J.P.B. Mota, J. Chromatogr. A 1180 (2008) 42.
[16] R.C.R. Rodrigues, R.J.S. Silva, J.P.B. Mota, J. Chromatogr. A 1217 (2010) 3382.
[17] J.M.M. Araújo, R.C.R. Rodrigues, M.F.J. Eusébio, J.P.B. Mota, J. Chromatogr. A 1217 (2010) 5407.
[18] T. Masuda, T. Sonobe, F. Matsuda, M. Horie, U.S. Patent No. 5,198,120, 1993.
[19] V. Mata, A.E. Rodrigues, J. Chromatogr. A 939 (2001) 23.
[20] E.V. Borges da Silva, A.E. Rodrigues, AIChE J. 52 (2006) 3794.
[21] E.A. Borges da Silva, A.E. Rodrigues, Sep. Sci. Technol. 43 (2008) 533.
[22] J.S. Hur, P.C. Wankat, Ind. Eng. Chem. Res. 44 (2005) 1906.
[23] J.S. Hur, P.C. Wankat, Ind. Eng. Chem. Res. 45 (2006) 1426.
[24] G. Ströhlein, L. Aumann, M. Mazzotti, M. Morbidelli, J. Chromatogr. A 1126 (2006) 338.
[25] L. Aumann, M. Morbidelli, European Patent EP 05405327.7, EP 05405421.8, 2005.
[26] L. Aumann, M. Morbidelli, Biotechnol. Bioeng. 98 (2007) 1043.
[27] L. Aumann, G. Ströhlein, M. Morbidelli, Biotechnol. Bioeng. 98 (2007) 1029.
[28] L. Aumann, M. Morbidelli, Biotechnol. Bioeng. 99 (2008) 728.
[29] T. Müller-Späth, L. Aumann, L. Melter, G. Ströhlein, M. Morbidelli, Biotechnol. Bioeng. 100 (2008) 1166.
[30] E. Valéry, H. Osuna-Sanchez, M. Bailly, World Patent WO 2009/122281 A1, 2007.
[31] M.F.J. Eusébio, Development of an universal interface for monitoring and control of chemical and biochemical processes, Ph.D. Thesis, Universidade Nova de Lisboa, Lisbon, Portugal, 2006 (in Portuguese).
[32] A. Abbood, C. Smadja, C. Herrenknecht, Y. Alahmad, A. Tchapla, M. Taverna, J. Chromatogr. A 1216 (2009) 3244.
[33] F. Gritti, G. Guiochon, J. Chromatogr. A 1028 (2004) 197.
[34] F. Gritti, G. Guiochon, J. Chromatogr. A 1038 (2004) 53.
[35] M. Mazzotti, G. Storti, M. Morbidelli, J. Chromatogr. A 769 (1997) 3.
[36] N. Jakobsson, M. Degerman, B. Nilsson, J. Chromatogr. A 1099 (2005) 157.
[37] M. Degerman, N. Jakobsson, B. Nilsson, J. Chromatogr. A 1113 (2006) 92.
[38] M. Degerman, N. Jakobsson, B. Nilsson, J. Chromatogr. A 1162 (2007) 41.
[39] G. Guiochon, S. Golshan-Shirazi, A. Katti, Fundamentals of Preparative and Nonlinear Chromatography, Academic Press, Boston, MA, 1994.
[40] D.M. Ruthven, Principles of Adsorption and Adsorption Processes, John Wiley, New York, NY, 1984.
[41] J.P.B. Mota, J.M.M. Arauújo, AIChE J. 51 (2005) 1641.
[42] J.M.M. Arauújo, R.C.R. Rodrigues, J.P.B. Mota, Ind. Eng. Chem. Res. 45 (2006) 5314.
[43] Araújo JMM, Rodrigues RCR, Mota JPB, J. Chromatogr. A 1132 (2006) 76.
[44] R.C.R. Rodrigues, J.M.M. Araújo, M.F.J. Eusébio, J.P.B. Mota, J. Chromatogr. A 1142 (2006) 69.
[45] E. Valéry, C. Morey, World patent WO 2007/101944 A2, 2007.